modeling of a near wake is to draw the mathematical analogy between a steady near-wake and an implosion wave generator. This analog remains valid when the pressure gradient term is included in Eq. (1). It is expected that the density and potential peaks in the wake would be less sharp with the pressure gradient taken into account, which is appropriate when $T_i \approx T_e$.

References

[1] Liu, V. C., "Ionospheric Gas Dynamics of Satellites and Diagnostic Probes," *Space Science Reviews*, Vol. 9, June 1969, p. 423.

[2] Liu, V. C., "On Ionospheric Aerodynamics," *Progress in Aerospace Sciences*, Vol. 16, 1975, p. 273.

[3] Gurevich, A. V., Pitaevskii, L. P., and Smirnova, V. V., "Ionospheric Aerodynamics," *Space Science Reviews*, Vol. 9, Sept. 1969, p. 805; also *Soviet Physics (Uspekhi)*, Vol. 12, 1970, p. 595.

[4] Alpert, J. L., "Wave-Like Phenomena in the Near-Earth Plasma and Interactions with Man-Made Bodies," *Handbuch der Physik*, edited by S. Flugge, Vol. 49/5, Springer-Verlag, Berlin, 1976, p. 217.

[5] Hester, S. D. and Sonin, A. A., "A Laboratory Study of the Wakes of Ionospheric Satellites," *AIAA Journal*, Vol. 8, June 1970, p. 1090.

[6] Fournier, G. and Pigache, D., "Wakes in Collisionless Plasma," *Physics of Fluids*, Vol. 18, Nov. 1975, p. 1443.

[7] Widner, M., Alexeff, I., and Jones, W. D., "Plasma Expansion into a Vacuum," *Physics of Fluids*, Vol. 14, April 1971, p. 795.

[8] Ying, S. J. and Liu, V. C., "An Extension of MacCormack's Method for Flows with Higher-Order Equations and in Different Configurations," *Computers and Fluids*, Vol. 6, Sept. 1978, p. 173.

[9] Ames, W. F., *Nonlinear Partial Differential Equations in Engineering*, Academic Press, New York, 1965, p. 66.

[10] Clemmow, P. C. and Dougherty, J. P., *Electrodynamics of Particles and Plasmas*, Addison-Wesley, Reading, Mass., 1969, p. 175.

J80-242

Marker Particle Velocity Perturbations in Compressible Flows over a Wavy Wall

G. D. Catalano*
Air Force Flight Dynamics Lab., Wright-Patterson AFB, Ohio

Introduction

A THEORETICAL investigation using a perturbation technique of the compressible flow of a contaminated gas over a wavy wall is made. Different behaviors of the marking particles are noted for subsonic and supersonic outer streams.

In a previous report[1] an analytical investigation of the steady motion of a dusty gas impinging at a right angle to a flat wall was made. The gas flow was assumed to be inviscid and incompressible. Also, the dust particles were assumed to be spherically shaped and not interact with one another. A perturbation technique was used to solve for the motion of the dust particles and the gas flow. The main conclusion reached was that the trajectories of the contaminant particles do not coincide with the streamlines of the gas flow to even first order. The dust particles are slow to respond to any change in the direction of flow. In the simple case of the impinging uniform stream, the dust particles tended to settle out of the flow.

The purpose of this Note is twofold. Initially, the general equations will be extended to the case when the flow is steady, isentropic, and compressible. The equations will then be applied to both subsonic and supersonic gas flows over a wavy wall. A perturbation technique will again be used.

Liepman and Roshko[2] have shown that the scalar form of the momentum equation for an isentropic flow is

$$u_i u_j \frac{\partial u_i}{\partial x_j} = a^2 \frac{\partial u_k}{\partial x_k}$$

where u_i and a are the velocity of the flow and the speed of sound, respectively. Next, consider the effects of the presence of dust particles on the flowfield. Saffman[3] used the following equations to represent the motion of an inviscid dusty gas:

$$\rho \frac{\partial u_i}{\partial t} + \rho u_j \frac{\partial u_i}{\partial x_j} = -\frac{\partial p}{\partial x_i} + KN(v_{pi} - u_i) \tag{1}$$

$$m \frac{\partial v_{pi}}{\partial t} + m v_{pj} \frac{\partial v_{pi}}{\partial x_j} = K(u_i - v_{pi}) \tag{2}$$

where v_{pi} is the particle velocity and N is the number density of the dust particles, each of mass m; K is the Stokes' coefficient of resistance; and ρ is the density of the gas. Combining Eqs. (1) and (2) and transforming into scalar form yields

$$a^2 \frac{\partial u_k}{\partial x_k} = u_i u_j \frac{\partial u_i}{\partial x_j} + \frac{f}{\tau} u_i (u_i - v_{pi}) \tag{3}$$

where $f = Nm/\rho$, and τ, the relaxation parameter, equals m/K.

Application

Consider a slightly disturbed uniform flow such that

$$u_1 = U_\infty + u_{c_1}, \quad u_2 = u_{c_2}, \quad u_3 = u_{c_3} \tag{4}$$

and the particle velocity is given by

$$v_{p_1} = u_1 + v_{d_1}, \quad v_{p_2} = u_2 + v_{d_2}, \quad v_{p_3} = u_3 + v_{d_3} \tag{5}$$

where u_{c_i} are perturbations due to a small disturbance and v_{d_i} are perturbations between the flow and particle velocities.

Neglecting terms containing squares of perturbation powers and all terms on the right-hand side in comparison with those on the left which contain no perturbation velocity yields

$$(1 - M_\infty^2) \frac{\partial u_1}{\partial x_1} + \frac{\partial u_2}{\partial x_2} + \frac{\partial u_3}{\partial x_3} = \frac{-fM_\infty^2}{\tau U_\infty} [v_{d_1}] \tag{6}$$

The equations of motion for the compressible flow of a dusty gas have been developed. The flow over a wavy wall in both the subsonic and supersonic regimes will now be analyzed.[2]

Consider the flow past a boundary of sinusoidal shape with the boundary specified by

$$x_2 - \epsilon \sin \alpha x_1 = 0 \tag{7}$$

where ϵ denotes the amplitude of the waves of the wall and $\ell = 2\pi/\alpha$, the wavelength.

Received Nov. 19, 1979; revision received Feb. 28, 1980. This paper is declared a work of the U.S. Government and therefore is in the public domain.

Index categories: Hydrodynamics; Computational Methods; Boundary Layers and Convective Heat Transfer—Laminar.

*Aerospace Engineer, Aerodynamics Division.

To a first-order approximation, the dust particle perturbation velocity[1] is given by

$$v_{d_i} = -u_{c_j}\frac{\partial u_{ci}}{\partial x_j} = \frac{-\tau}{2}\frac{\partial}{\partial x_i}\left(\frac{\partial \phi}{\partial x_j}\right)^2 \tag{8}$$

This equation is derived from Saffman's[3] development. The flow is treated as steady and inviscid. The dust in the flow is assumed to be spherically shaped and the individual dust particles do not interact with each other. The concentration of the contaminant is required to be low; i.e., 1 part/1000 based on volume.

Recall

$$\phi(x_1,x_2) = -\frac{U\epsilon}{\lambda}e^{-x_2\alpha\lambda}\cos\alpha x_1 \tag{9}$$

where

$$\lambda = (1-M_\infty^2)^{1/2}$$

Then,

$$v_{d_1} = \frac{-\tau}{2}\frac{\partial}{\partial x_1}\left[\left(\frac{\partial \phi}{\partial x_1}\right)^2 + \left(\frac{\partial \phi}{\partial x_2}\right)^2\right] \tag{10}$$

So

$$v_{d_1} = \frac{-\tau}{2}\left[U_\infty^2\epsilon^2\alpha^3 e^{-2x_2\alpha\lambda}\sin 2\alpha x_1\left(\frac{1}{\lambda^2}-1\right)\right] \tag{11}$$

Similarly,

$$v_{d_2} = \frac{-\tau}{2}\frac{\partial}{\partial x_2}\left[\left(\frac{\partial \phi}{\partial x_1}\right)^2 + \left(\frac{\partial \phi}{\partial x_2}\right)^2\right] \tag{12}$$

or

$$v_{d_2} = \tau\lambda U_\infty^2\epsilon^2\alpha^3 e^{-2x_2\alpha\lambda}\left(\frac{1}{\lambda^2}\sin^2\alpha x_1 + \cos^2\alpha x_1\right) \tag{13}$$

The maximum dust perturbation occurs when $x_2 = 0$. Then,

$$v_{d_1} = -\tau/2U_\infty^2\epsilon^2\alpha^3\left(\frac{1}{\lambda^2}-1\right)[\sin^2\alpha x_1] \tag{14}$$

and

$$v_{d_2} = \tau\lambda U_\infty^2\epsilon^2\alpha^3\left[\frac{\sin^2\alpha x_1}{\lambda^2} + \cos^2\alpha x_1\right] \tag{15}$$

A better understanding of the nature of the dust particle behavior can be obtained by comparing the maximum contaminant velocity change to the maximum perturbation due to the wavy wall. So for $\alpha x_1 = 0$ and noting $\sin^2\alpha x_1/\sin\alpha x_1 = 2\cos\alpha x_1$, then

$$\frac{v_{d_1}}{u_{c_1}} = -\tau U_\infty\epsilon\alpha^2\left(\frac{1}{\lambda}-\lambda\right) \tag{16}$$

and

$$\frac{v_{d_2}}{u_{c_2}} = \tau U_\infty\epsilon\alpha^2\left(\frac{1}{\lambda}\right) \tag{17}$$

For the supersonic case, the velocity components of the dust particle are:

$$v_{d_1} = \frac{+\tau}{2}U_\infty^2\epsilon^2\alpha^3\left(\frac{1}{\lambda^2}+1\right)\sin 2\alpha(x_1-\lambda x_2) \tag{18}$$

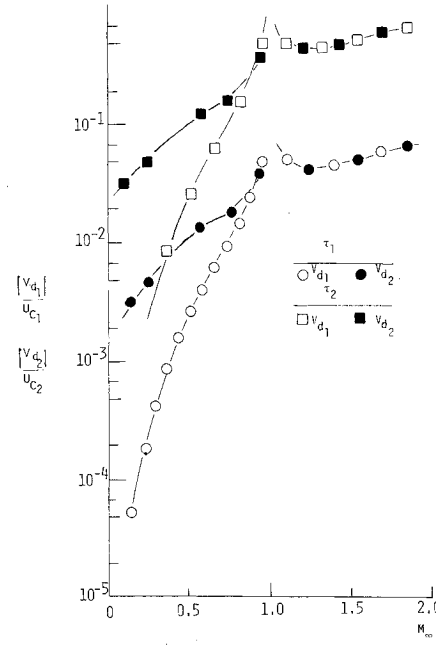

Fig. 1 Longitudinal and transverse velocity perturbations: $\tau_1 = 1.193\times10^{-5}$ s, $\tau_2 = 1.193\times10^{-4}$ s.

$$v_{d_2} = -\frac{\tau\lambda}{2}U_\infty^2\epsilon^2\alpha^3\left(\frac{1}{\lambda^2}+1\right)\sin 2\alpha(x_1-\lambda x_2) \tag{19}$$

The maximum dust perturbation occurs when $2\alpha\ (x_1 - \lambda x_2) = \pi/2$ or $x_1 - \lambda x_2 = \pi/4\alpha$ for any λ. Then,

$$v_{d_1} = \frac{\tau}{2}U_\infty^2\epsilon^2\alpha^3\left(\frac{1}{\lambda^2}+1\right) \tag{20}$$

$$v_{d_2} = -\frac{\lambda\tau}{2}U_\infty^2\epsilon^2\alpha^3\left(\frac{1}{\lambda^2}+1\right) \tag{21}$$

Again, comparing the maximum contaminant velocity change to the maximum perturbation due to the wavy wall yields

$$\frac{v_{d_1}}{u_{c_1}} = \frac{+\tau}{2}U_\infty\epsilon\alpha^2\left(\frac{1}{\lambda}+\lambda\right) \tag{22}$$

$$\frac{v_{d_2}}{u_{c_2}} = \frac{-\tau}{2}U_\infty\epsilon\alpha^2\left(\frac{1}{\lambda}+\lambda\right) \tag{23}$$

Results

In Fig. 1, the values of the ratio of the dust perturbation velocity to the perturbation due to the wavy wall are plotted vs Mach number for two values of the relaxation parameter τ. Values chosen for the parameters are: $\epsilon = 0.1$ m, $\alpha = 2\pi/$m, $\tau_1 = 1.193\times10^{-5}$ s, and $\tau_2 = 1.193\times10^{-4}$ s.

Several interesting observations can be made through examination of the data presented in Fig. 1. Notice that the assumption with reference to the dust perturbation velocity being a first-order term compared with the wall velocity perturbation is valid for all values of Mach number (i.e., $M_\infty \neq 1$) for the smaller value of the relaxation parameter τ. The approximation becomes increasingly suspect as the dust concentration is increased.

A second observation concerns comparison of the dust perturbation velocity components in the longitudinal and in the transverse direction. For a subsonic freestream, the transverse dust perturbation velocity is approximately an

order of magnitude larger than the longitudinal velocity perturbation. For a supersonic freestream, the maximum dust perturbation velocity is the same in both the longitudinal and in the transverse directions.

References

[1] Catalano, G. D., "Flow of a Marking Particle in a Two Dimensional Stagnation Region," Air Force Flight Dynamics Lab. Tech. Memo. No. 78-21, 1977.

[2] Liepman, H. W. and Roshko, A., "Small Perturbation Theory," *Elements of Gasdynamics*, Wiley, New York, 1957, pp. 202-215.

[3] Saffman, P. G., "The List on a Small Sphere in a Slow Shear Flow," *Journal of Fluid Mechanics*, Vol. 22, Pt. 2, June 1965, pp. 385-400.

J80 - 243

20006
20019

Sullivan's Two-Celled Vortex

Fred W. Leslie* and John T. Snow†
Purdue University, West Lafayette, Ind.

IN Ref. 1, Sullivan presented an exact solution to the Navier-Stokes equations for a three-dimensional axisymmetric two-celled vortex. In the outer cell of this solution, fluid spirals inward from a large radius on stream surfaces that gradually turn upward from concentric cylindrical sheaths about the axis. Free-slip conditions are assumed on the lower surface with diffusive processes working only in the radial direction to balance the inward transport of angular momentum by the radial-axial velocity field. The inner cell consists of downward flow immediately about the axis. At the base of the vortex, this downward flow is turned outward and then moves upward with the swirling outer flow. Rotation within this cell is maintained by viscous diffusion.

In a cylindrical coordinate system, the radial, axial, and tangential velocity components and the pressure deficit are given by

$$u(r) = -ar + (6\nu/r)\,[1-\exp(-ar^2/2\nu)] \tag{1}$$

$$w(r,z) = 2az[1-3\exp(-ar^2/2\nu)] \tag{2}$$

$$v(r) = (\Gamma/2\pi r)\,[H(ar^2/2\nu)/H(\infty)] \tag{3}$$

$$\Delta p(r,z) \equiv p(r,z) - p(0,z) = -\frac{\rho}{2}\left\{4a^2z^2 + a^2r^2 + \frac{36\nu^2}{r^2}\left[1-\exp(ar^2/2\nu)\right]^2\right\} + \rho\int_0^r \frac{v^2}{r}\,dr \tag{4}$$

where a is the convergence strength of the flow-through field, ρ the fluid density (assumed constant), Γ the circulation at infinite radius, ν the kinematic viscosity, and H a function given by

$$H(x) = \int_0^x \exp\left\{-t + 3\int_0^t [(1-e^{-\tau})/\tau]\,d\tau\right\}dt \tag{5}$$

Received Dec. 10, 1979; revision received Feb. 19, 1980.

Index categories: Viscous Nonboundary-Layer Flows; Hydrodynamics.

*Postdoctoral Research Associate, Dept. of Geosciences.
†Assistant Professor, Dept. of Geosciences.

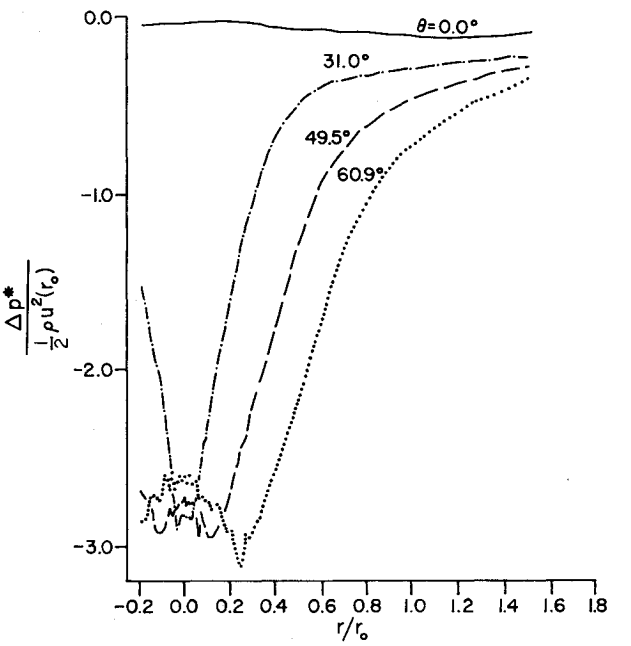

Fig. 1 Pressure profiles measured in the Purdue tornado simulator for various swirl angles.

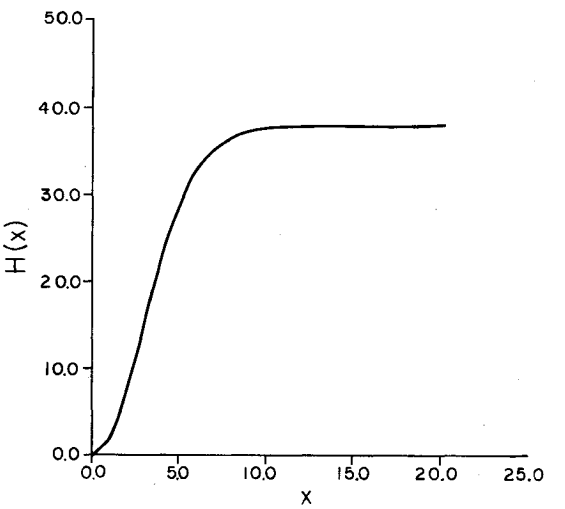

Fig. 2. $H(x)$ vs x, as given by Eq. (5).

Sullivan presented plots of the axial and tangential velocities as functions of radius, and compared the flow described by Eqs. 1-4 with the earlier parallel solution by Burgers[2,3] and Rott[4,5] for a one-celled vortex. Here, Sullivan's note is extended by providing a tabulation of $H(x)$, by evaluating Eq. (5), and by presenting plots of the surface pressure deficit. This work was motivated by recent measurements by the authors[6,7] of the wall static pressure fields beneath two-celled vortices generated in laboratory tornado simulators.

In order to better understand the behavior of the vortex core pressure, it is more informative to measure $p(r,0) - p(r_{ref},0) \equiv \Delta p^*(r)$ (where r_{ref} is a reference radius in the far-field of the flow) than Sullivan's $\Delta p(r) = p(r,0) - p(0,0)$. These two different representations of pressure deficit differ only by the amount $p(0,0) - p(r_{ref},0)$. A set of radial pressure profiles measured in the Purdue tornado simulator is shown in Fig. 1. The radial position is nondimensionalized by r_0, a characteristic radial scale of the apparatus. Similarly, the pressure deficit is nondimensionalized by $1/2\ \rho u^2(r_0)$. The profiles were measured for a fixed geometry and volume flow rate. Each profile in the set is characterized by a selected value of far-field angular momentum. This is indicated by the given